

# **Non-Covalent Functionalisation of Carbon Nanotubes and Graphene**

## **Introduction**

In previous chapters, I have discussed methods of fabricating carbon nanotube and graphene devices and then shown that they are sensitive to environmental changes in a saline solution. However, for specific sensing, the devices require (bio)chemical functionalisation. Instead of responding to stimuli themselves, the sensing signal is picked up by attached receptors. The devices then act as passive transducers for the received signal. Receptors previously used with carbon nanotube and graphene devices include aptamers [ @Khan2021; @Nguyen2021; @Shkodra2021; @Nekrasov2021; @Mishyn2022; @Cassie2023] and a range of proteins [ @Lerner2014; @Ahn2020; @Tong2020; @Wang2020], including animal odorant receptors [ @Goldsmith2011; @Lee2018; @Murugathas2019b; @Murugathas2020; @Moon2020; @Yoo2022]. A common approach to attaching receptors to the transducer involves the use of a linker molecule to tether the receptor to the transducer. Verifying that this linker molecule is bridging between the transducer and the receptor element is important for a complete understanding of the behaviour of these sensors. This verification involves providing evidence for effective attachment of linker molecule to the transducing device channel, then showing successful tethering of odorant receptors and other biomolecules to the attached linker molecule.

This chapter therefore takes some time exploring the following selection of available linker molecules for specific biosensing: 1-Pyrenebutanoic Acid N-Hydroxysuccinimide Ester (PBASE), 1-Pyrenebutyric Acid (PBA), Pyrene-PEG-NTA (PPN) and Pyrene-PEG-Biotin (PPB). The linker molecules used are discussed in detail, and numerous hurdles to successful functionalisation via linker molecules are identified and addressed. Next, it looks at verifying that the odorant receptor proteins of interest have specifically attached to these linker molecules. The experimental parameters used for both the attachment of linker molecules and receptor proteins are also varied, and the impact of these variations on successful functionalisation is investigated via Raman spectroscopy, fluorescence microscopy and electrical characterisation.

## **Non-Covalent Bonding and $\pi$ -Stacking**

Linker molecules may be attached via covalent or non-covalent bonding to carbon nanomaterials, such as carbon nanotubes and graphene. Covalent bonding is stronger than non-covalent bonding, and therefore gives a more permanent attachment between linker molecules and the transducer. However, non-covalent bonding has the advantage of having less of an impact on the structure of a nanomaterial than covalent bonding, meaning non-covalent bonding is less likely to negatively affect the electrical properties of the transducer [ @Long2012; @DiCrescenzo2014; @Wang2020; @Khan2021; @Mishyn2022]. For example, one group found covalent bonding of diazonium linker caused a  $\sim 50\%$  drop in graphene channel mobility [ @Lerner2014]. In comparison, only a  $\sim 5\%$  drop in mobility was seen for attachment of

a mixture of linkers containing pyrene to a graphene channel via non-covalent  $\pi$  stacking [@[Thodkar2021]].

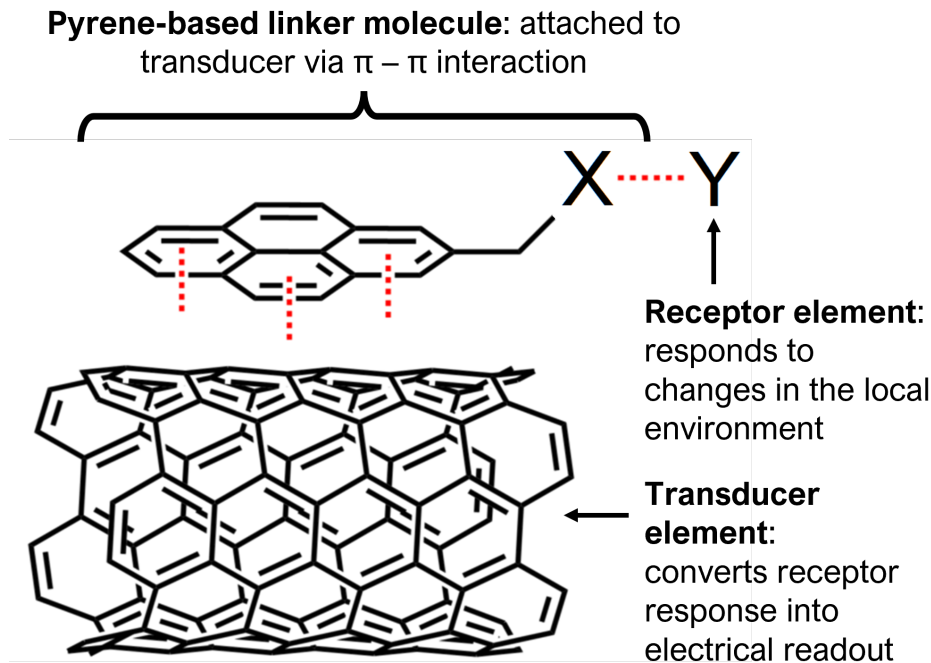


Figure 1: Attachment of pyrene-based linker molecule pyrene-X and receptor Y to a carbon nanotube, representing the transducer element of a field-effect transistor. Source: Adapted from [@[Carbonnanotube]].

$\pi$ -stacking or  $\pi - \pi$  interaction is often used to describe a type of non-covalent bonding which occurs due to dispersion forces between unsaturated polycyclic molecules [@[Perez2015]]. It has been argued that this label is unhelpfully specific and a misrepresentation of what can be simply classed as a type of Van Der Waals bonding [@[Martinez2012]; [@[Perez2015]]. However, as the use of the term is widespread in the literature, it is also used here for the sake of clarity. Carbon nanotubes and graphene consist of a network of carbon atoms attached to each other by  $sp^2$  hybrid orbitals in a polycyclic structure. They are therefore able to strongly interact with linker molecules with aromatic moieties, such as pyrene [@[Hermanson2013-16]; [@[Perez2015]; [@[Mishyn2022]]. Figure 1 is a visual demonstration of the relationship between the pyrene-based linker molecule with the transducer and receptor elements. A wide range of pyrene-based linker molecules have been used for non-covalent modification of carbon nanotubes and graphene [@[Zhou2019]].  $\pi$ -stacking with pyrene is the bonding mechanism underlying all the functionalisation processes in this thesis.

## Attachment of 1-Pyrenebutanoic Acid N-Hydroxysuccinimide Ester

## Comparing Attachment Methods

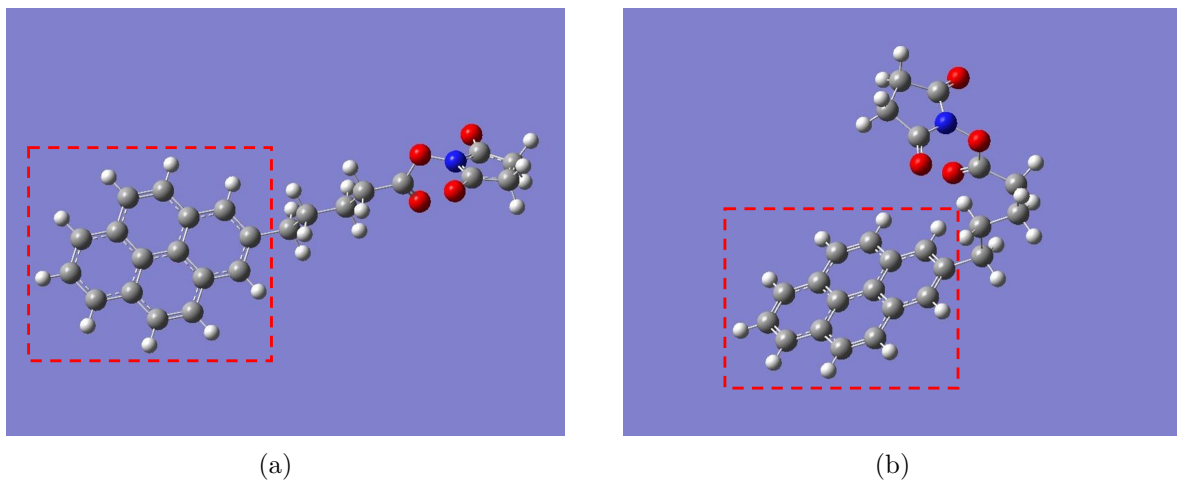


Figure 2: Two conformations of PBASE molecule with geometry optimised via *ab initio* calculations performed with Gaussian 16 software [@g16]. White balls correspond to hydrogen, grey to carbon, red to oxygen and blue to nitrogen. The pyrene moiety is highlighted in the image with a red dashed outline.

1-pyrenebutanoic acid N-hydroxysuccinimide ester (also known commercially and in the literature both as 1-pyrenebutyric acid N-hydroxysuccinimide ester and 1-pyrenebutanoic acid succinimidyl ester; acronyms include PBASE, PBSE, PyBASE, PASE, PYSE, PSE, Pyr-NHS and PANHS) is a aromatic molecule commonly used for tethering biomolecules to the carbon rings of graphene and carbon nanotubes. Using computational modelling, two locally stable molecular conformations were found to exist, a straight (Figure 2a) and bent (Figure 2b) structure. The conformation in Figure 2a has a Hartree-Fock energy of -3427728.67 kJ/mol, while the conformation in Figure 2b has a Hartree-Fock energy of -3427729.66 kJ/mol. The difference between computed Hartree-Fock energies is 1.0 kJ/mol, small enough that the existence of both molecular conformations is physically feasible. Similar straight and bent structures have previously been modelled for PBASE attached to graphene [@Oishi2022].

```

knitr::opts_chunk$set(echo = FALSE)
library(knitr)

pbase_table <- read.csv("tables/ch7/pbase_table.csv", sep=",")
pbase_table <- pbase_table[rowSums(is.na(pbase_table)) == 0,]

knitr::kable(pbase_table,
             col.names = c("Solvent",
                           "Channel",
                           "Conc. (mM)",
                           "Incubation type",
                           "Time (hr)",
                           "Rinse steps",
                           "References"), format = "simple")

```

Table 1: Comparison of PBASE functionalisation processes used for immobilisation of proteins and aptamers onto carbon nanotubes and graphene. Experimentally optimised variables are marked with a star (\*). Blank entries indicate there was no mention of the parameter in a particular paper.

Solvent	Channel	Conc. (mM)	Incubation type	Time (hr)	Rinse steps	References
DMF	CNT	5	Immersed	1	PBS	Maehashi, 2007. [?]
		6	Immersed	1	DMF, PBS	García-Aljaro, 2010. [?]
		6	Immersed	1	DMF	Chen, 2001. [?]
		6	Immersed	1	DMF	Cella, 2010. [?]
		6	Immersed	1	DMF	Das, 2011. [?]
		6	-	2	DMF	Besteman, 2003. [?]
Graphene	-	-	-	2	DMF	Tsang, 2019. [?]
		-	-	20	-	Wiedman, 2017. [?]
		0.2	Immersed	20	DMF, IPA, DI water	Gao, 2018. [?]
		1	Dropcast	6	DMF, IPA, DI water	Nekrasov, 2021. [?]
		5	Immersed	1	DMF, DI water	Hwang, 2016. [?]
		5*	Immersed	3*	DMF	Hao, 2020. [?]
		5	Immersed	4*	DMF, DI water	Mishyn, 2022. [?]
		6	Dropcast	2	DMF, DI water	Nur Nasufiya, 2020. [?]
		10	Dropcast	2	DMF, DI water	Campos, 2019. [?]
		10	Immersed	2	DMF, PBS	Kuscu, 2020. [?]
		10	Immersed	1	DMF	Xu, 2017. [?]
		10	Immersed	12	DMF, EtOH, DI water	Khan, 2020. [?]

Solvent	Channel	Conc. (mM)	Incubation type	Time (hr)	Rinse steps	References
Methanol	CNT	1	Immersed	1	MeOH, DI water	Zheng, 2016. [?]
		1	Immersed	2	MeOH	Kim, 2009. [?]
		100	Dropcast	1	DI water	Yoo, 2022. [?]
	Graphene	5	Immersed	2	-	Sethi, 2020. [?]
		5	Immersed	1	MeOH, PBS	Ohno, 2010. [?]
	DMSO	10	-	1	DI water	Lopez, 2015. [?]
		10	Immersed	1	PBS	Strack, 2013. [?]

The pyrene moiety, highlighted with a red dashed outline in Figure 2a-b, non-covalently bonds to the carbon rings of the carbon nanotube and graphene surface. The N-hydroxysuccinimide (NHS) ester group, seen on the right-hand side of Figure 2, is highly reactive with amine groups. It can undergo a nucleophilic substitution reaction with amines attached to proteins or aptamers, tethering these biomolecules via an amide or imide bond [@Chen2001; @Hermanson2013-16; @Hermanson2013-3; @Mishyn2022].

The non-covalent functionalisation of proteins onto a single-walled carbon nanotube using PBASE was first reported by Chen *et al.* in 2001 [@Chen2001]. Two successful methods for protein functionalisation and immobilisation were reported, with the only differences being the solvent used to dissolve the PBASE powder (DMF, methanol) and the final concentration of the resulting solutions (6 mM, 1 mM respectively). PBASE powder appears to dissolve poorly in methanol at higher concentrations, which might explain the use of different concentrations of PBASE in each solvent. An extensive comparison of methods used in the literature for PBASE functionalisation of carbon nanotube and graphene devices with aptamers and proteins is given in Table 1. Several listed works directly cite Chen *et al.* when discussing functionalisation with PBASE [@Besteman2003; @Cella2010; @Campos2019; @Zheng2016; @Ohno2010]. The other works listed do not explicitly reference Chen *et al.* in their methodology; however, the frequency of methods detailing the use of 6 mM PBASE in dimethylformamide (DMF) and 1 mM PBASE in methanol indicate that these processes are largely copying the process used by Chen *et al.*.

However, it is also apparent from Table 1 that there is a large degree of variation in the methods used for PBASE functionalisation. Various electrical characterisation, microscopy and spectroscopy techniques have been used to demonstrate successful functionalisation. Until recently, there has been little justification provided for the selection of variables used in the functionalisation procedure (e.g. length of time submerged in solvent containing PBASE), despite the wide-ranging use of this process in the literature [@Hinnemo2017; @Zhen2018; @Wang2020]. This is surprising, given that the sensitivity of functionalised devices is considered to be closely related to the density of surface functionalisation [@White2008; @Hermanson2013-3; @Chen2014]. Furthermore, a detailed investigation of PBASE functionalisation process variables has only been undertaken for graphene-based devices [@Zhen2018; @Hao2020; @Wang2020; @Mishyn2022].

Zhen *et al.* [@Zhen2018], Wang *et al.* [@Wang2020] and Mishyn *et al.* [@Mishyn2022] have all claimed that carefully tuning the surface concentration of PBASE is required to avoid multilayer coverage of the graphene surface, as this negatively impacts sensing. Mishyn *et al.* [@Mishyn2022] used cyclic voltammetry to demonstrate that less receptor attachment to the graphene surface occurs when multiple layers of PBASE are present. However, none of these groups have presented analyte sensing results from their functionalised graphene devices. In contrast, Hao *et al.* [@Hao2020] found that maximising the PBASE surface coverage of a channel resulted in more sensitive aptameric sensing, thereby reaching the opposite conclusion. The inconsistency in these recent findings mean more work is needed to understand the PBASE functionalisation process to achieve optimal biosensor sensitivity. It may also be the case that

a specific functionalisation process is required for optimal sensitivity with the use of a specific type of receptor.

Once fastened to a bioreceptor via an amide or imide bond, the attachment to the linker molecule is not easily broken. However, prior to use in functionalisation processes, the NHS ester may react with any water present (hydrolysis). This reaction converts PBASE to 1-pyrenebutyric acid (PBA), leaving it unavailable to react further with amine groups [@Hermanson2013-3; @Hermanson2013-5; @Mishyn2022]. If the amine group functionalisation is performed within a  $\sim$  1 hour period, with a high concentration of bioreceptor used at close to neutral pH, competing hydrolysis should not have a significantly adverse impact on the functionalisation process [@Hermanson2013-3]. However, if PBASE is exposed to water during storage over a significant length of time, the presence of 1-Ethyl-3-(3-dimethylaminopropyl)carbodiimide (EDC) can be used to restore the NHS ester and enable the substitution reaction to take place (see discussion of PBA/EDC in Section ).

### Examining 1-Pyrenebutanoic Acid N-Hydroxysuccinimide Ester Purity

I purchased PBASE from two suppliers, Sigma-Aldrich and Setareh Biotech. Sigma recommended DMF and methanol as suitable solvents for dissolving PBASE, alongside chloroform and dimethyl sulfoxide (DMSO). Setareh Biotech indicated methanol can be used for dissolving PBASE. The two suppliers had conflicting information for suitable storage of PBASE, with Sigma recommending room temperature storage while Setareh Biotech recommends storage of -5 to -30°C and protection from light and moisture. I used nuclear magnetic resonance (NMR) spectroscopy to verify the purity of PBASE from various suppliers. As water can react with PBASE to form unwanted byproducts, it appears that protection from moisture is particularly important. A particular emphasis was placed on detecting water presence in the received samples, considering the long travel time of the PBASE with uncertain storage conditions.

Figure 3 compares the shapes of hydrogen NMR spectra of PBASE from each supplier when dissolved in deuterated DMSO, alongside a blank deuterated DMSO spectrum. Both PBASE samples possessed characteristic chemical shift features between 2.1 – 2.2 ppm, 2.8 – 2.9 ppm, and 3.4 – 3.5 ppm. These chemical shifts roughly correspond to those seen in previous NMR spectra for PBASE [@NMR2]. The feature at 2.50 ppm represents the deuterated DMSO solvent, while the single peak between 3.3 – 3.4 ppm represents the water present in the sample. By comparing the area of these peaks, a rough estimate of the amount of water originally present in the PBASE sample can be obtained. The H<sub>2</sub>O:DMSO ratio is 1:7 in the blank spectrum, but  $\sim$  1:3 in the provided samples, possibly indicating the introduction of water to the PBASE during production or storage. However, DMSO is strongly hygroscopic and slight differences in DMSO storage time, as well as differences in humidity during sample preparation, may have had a significant impact on this result [@Lebel1962]. Other impurities are also seen on both PBASE spectra, though their small size indicates they make up only a small percentage of each sample. Strack *et al.* [@Strack2013] recommend leaving frozen

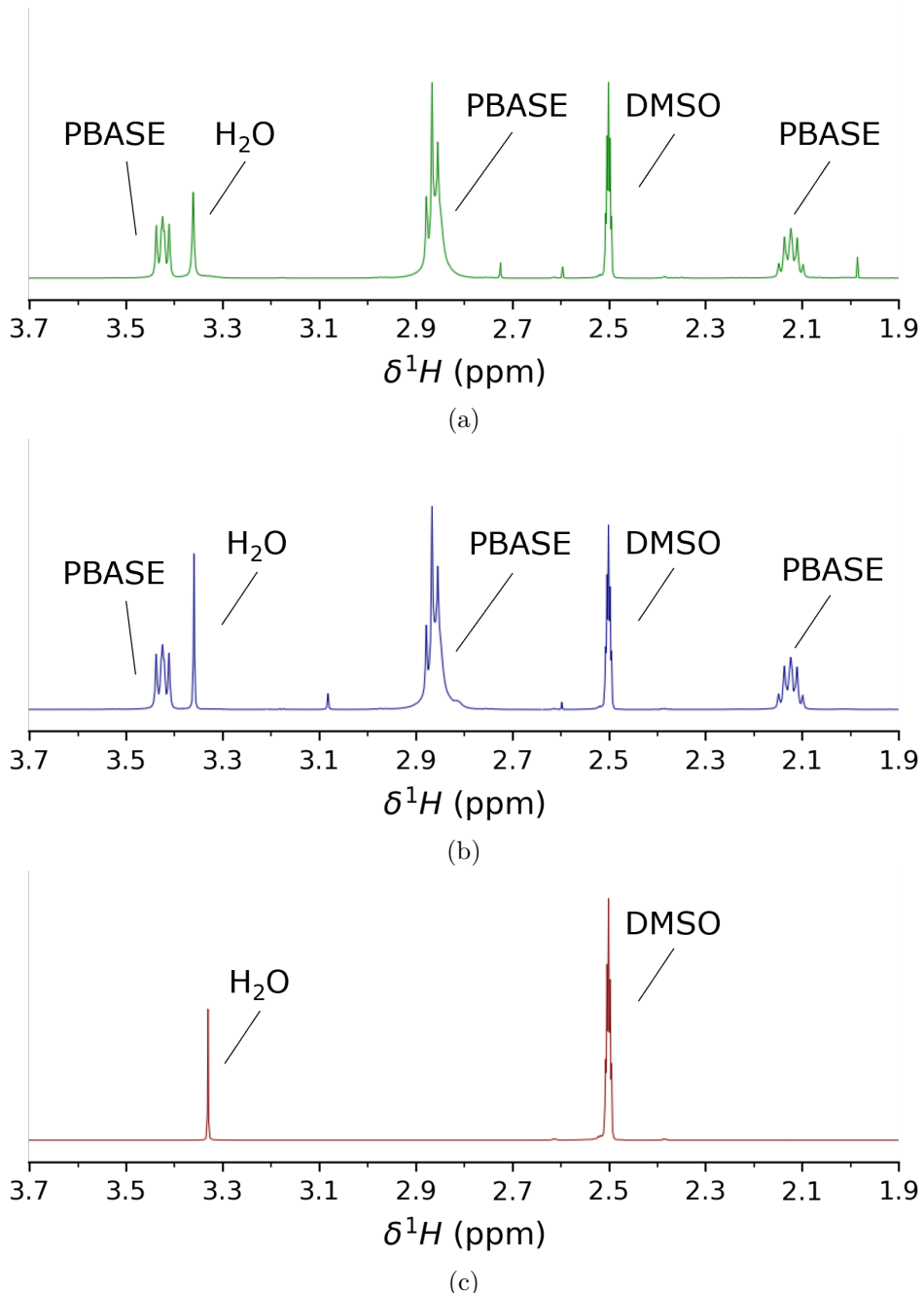


Figure 3:  $^1\text{H}$  Nuclear Magnetic Resonance (NMR) spectra, performed with  $\text{DMSO-d}_6$  used as the NMR solvent. (a) and (b) show NMR spectrum for commercially purchased PBASE, from Sigma-Aldrich and Setareh Biotech respectively, while (c) shows the blank spectrum taken with only  $\text{DMSO-d}_6$  present. Spectra were taken by Jennie Ramirez-Garcia, School of Chemical and Physical Sciences, Te Herenga Waka - Victoria University of Wellington. Unlabelled peaks correspond to sample impurities.

PBASE at room temperature for 15 minutes before exposing it to air to prevent condensation near the PBASE, as this can cause unnecessary  $H_2O$  contamination.

## Electrical Characterisation

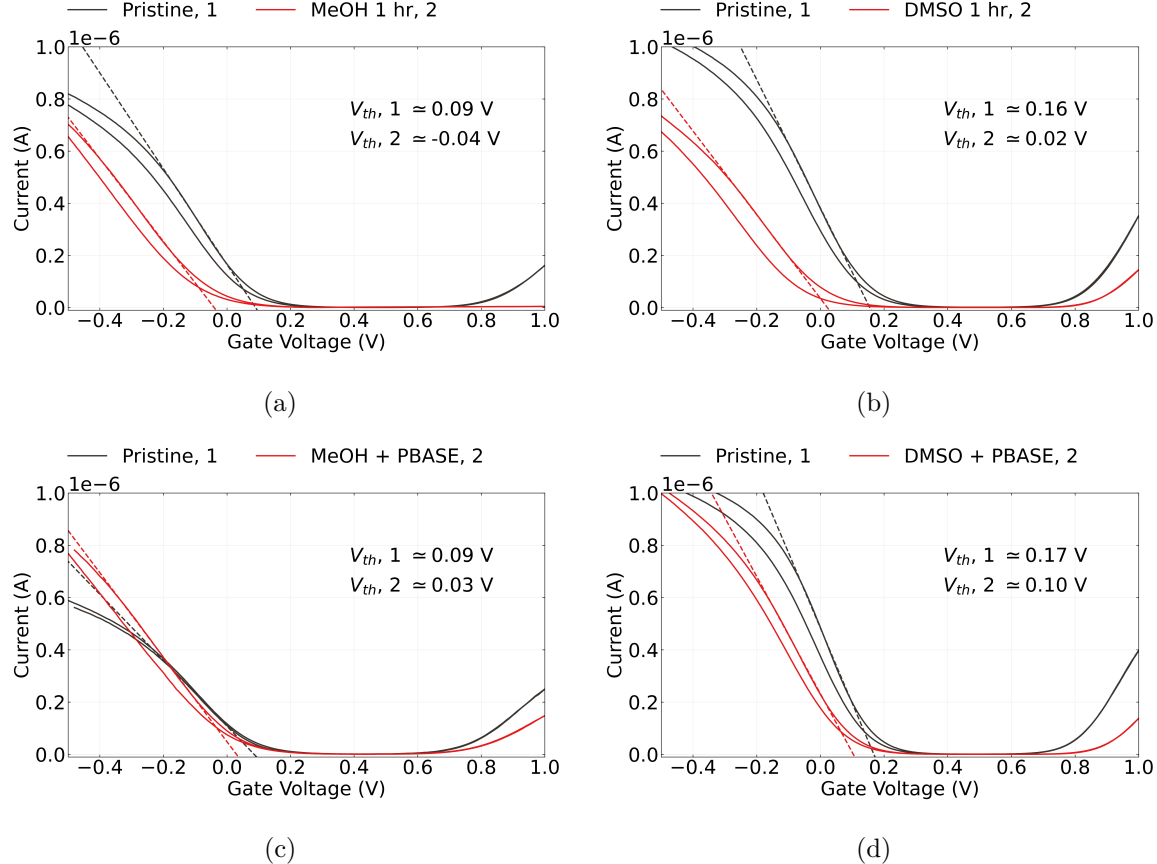


Figure 4: The electrical transfer characteristics of carbon nanotube transistors ( $V_{ds} = 100$  mV) before and after being submerged in methanol (a) or dimethyl sulfoxide (b) for one hour and subsequently rinsed with deionised water. The change in characteristics of similar transistor channels after being submerged in these same solvents containing 1 mM PBASE for one hour and then rinsed are shown in (c) and (d) respectively. Average threshold voltages for each transfer characteristic curve are also shown (taking the average of forward and reverse sweep values).

The electrical characteristics of the carbon nanotube or graphene transistor are often used to verify successful functionalisation and make a statement about the effect of chemical modification on the channel. However, this verification usually does not account for the effect

of the solvent on the transistor channel. Figure 4a and Figure 4b show that by exposing a steam-deposited carbon nanotube network channel to solvents commonly used in PBASE functionalisation processes (Table 1), such as methanol (MeOH) or dimethyl sulfoxide (DMSO), a significant negative shift in channel threshold voltage occurs even after thorough rinsing with deionised water. Besteman *et al.* reported observing a similar effect from prolonged exposure of a single carbon nanotube to dimethylformamide (DMF) [@Besteman2003]. It appears that the carbon nanotubes have adsorbed solvent which persists even after device cleaning. From the shape of the change in the transfer curve, it seems the residual polar solvent molecules capacitively gate the channel [@Artyukhin2006; @Heller2008].

Furthermore, using the same characterisation process as in this work, Murugathas *et al.* [@Murugathas2019b] showed that  $\pi$ -stacking of PBASE onto a solvent-deposited carbon nanotube network had little effect on channel threshold voltage, implying the presence of PBASE had not significantly influenced channel gating [@Murugathas2019b]. However, they did observe a slight increase in channel conductance after PBASE functionalisation. In Figure 4, a slight increase in channel conductance post-functionalisation is observed for both Figure 4c and Figure 4d when compared to the solvent-only case in Figure 4a and Figure 4b. This result implies that the presence of PBASE molecules increases channel mobility and therefore conductance [@Heller2008].

Capacitive gating results from dense coverage of adsorbed molecules on the carbon nanotube surface which have a low permittivity relative to the surrounding electrolyte [@Heller2008]. The relative permittivity of MeOH and DMSO are  $\sim 33$  [@Mohsen-Nia2010] and  $\sim 47$  [@Hunger2010] respectively, which are both much lower than the relative permittivity of phosphate buffer saline,  $\sim 80$  [@Shkodra2021]. From Figure 4a and Figure 4b, the threshold shift values found resulting from exposure to each solvent, taking the average of forward and reverse sweep values from a single device, were  $\Delta V = -0.15 \pm 0.02$  V and  $\Delta V = -0.15 \pm 0.01$  V for MeOH and DMSO respectively. The average threshold shift value for a second device exposed to MeOH was  $\Delta V = -0.16 \pm 0.02$  V, indicating that this threshold shift result is reproducible. The threshold voltage shifts in Figure 4c and Figure 4d from the pristine are small compared with the devices exposed to solvent only - this is likely due to the effect of increased conductance from the PBASE competing with the gating effect from the residual solvent.

The absorption of organic solvent by the carbon nanotube network has unknown but potentially negative implications for biosensor functionalisation. Use of organic solvents in functionalisation can also attack the encapsulation layer of devices, promoting gate current leakage. In light of these issues, recent work has begun to explore alternative aqueous-based methods for functionalisation of biosensors [@Khan2021]. The discussion here also illustrates the importance of considering each substance used when electrical characterising a device to verify if functionalisation has worked. The qualitative presence of a change in characteristics (or lack of one) over the full process is not sufficient to make conclusive remarks regarding successful functionalisation. A full set of electrical control measurements are required for an understanding of electronic changes occurring during the functionalisation process, in the manner of

Besteman *et al.* [@Besteman2003].

Table 2: Comparison of 1-pyrenebutyric acid (PBA) functionalisation processes used for immobilisation of proteins, enzymes and aptamers onto carbon nanotubes and graphene. 1-ethyl-3-(3-dimethylaminopropyl) carbodiimide hydrochloride (EDC) and NHS were co-mingled in buffer/electrolyte solution or DI water in each process - some papers used N-hydroxysulfosuccinimide instead of N-hydroxysuccinimide, and both compounds are abbreviated as NHS in this table for simplicity. Device exposure times to each solution are shown next to the solution concentration. Blank entries indicate there was no mention of the parameter in a particular paper. <sup>†</sup>PEG or PEG pyrene were used to reduce non-specific binding. <sup>††</sup>Several pyrene-based linkers were compared and PBA gave an optimal functionalisation result.

Solvent	Channel	PBA (mM)	Time (hr)	EDC (mM)	NHS (mM)	Time (min)	References
DMF	Graphene	0.6	1	-	-	120	Gao, 2016 <sup>†</sup> . [?]
		5	2	2	5	30	Mishyn, 2022. [?]
	CNT	100	3	200	-	30	Min, 2012. [?]
	Graphene, CNT	7.6	2	8	20	120	Xu, 2014. [?]
DI water	CNT	-	-	32	12	Overnight	Pacios, 2012 <sup>†</sup> . [?]
Ethanol	CNT	1	1	100	100	20	Filipiak, 2018 <sup>†</sup> . [?]
Acetonitrile	Graphene	1	1	400	100	60	Tong, 2020 <sup>††</sup> . [?]
Borax	CNT	2	24	2.5	-	1080	Liu, 2011 <sup>†</sup> . [?]
DMSO	Graphene	5	1	50	50	90	Fenzl, 2017. [?]

## Attachment of 1-Pyrenebutyric Acid

### Comparing Attachment Methods

Another linker molecule that can be used to attach receptor molecules to a carbon nanotube or graphene channel is 1-pyrenebutyric acid (PBA or PyBA). As with PBASE, the pyrene group of PBA has a  $\pi$  interaction with the carbon rings of the channel surface. It is possible to react PBA with 1-ethyl-3-(3-dimethylaminopropyl) carbodiimide hydrochloride (EDC or EDAC) to form an *O*-acylisourea intermediate, which can then react with an amine group on a biomolecule and form an amide bond [Sehgal1994; Hermanson2013-4]. The water solubility of EDC means that, unlike PBASE, it is possible to functionalise with EDC dissolved in water rather than in an organic solvent. However, like PBASE, EDC and the *O*-acylisourea intermediate are prone to hydrolysis, especially in acidic conditions. Therefore, like PBASE, it should be stored at  $-20^{\circ}\text{C}$ , and warmed to room temperature to prevent condensation build-up, since exposure to condensation will hydrolyse the reagent [Hermanson2013-4]. Furthermore, by adding N-Hydroxysuccinimide (NHS) or N-hydroxysulfosuccinimide (sulfo-NHS) to the reaction vessel, PBASE is formed as an active intermediate, which is less prone to hydrolysis and increases the PBA/EDC reaction yield [Sehgal1994; Hermanson2013-4; Hermanson2013-14].

A full comparison of functionalisation procedures used for linking carbon nanotube and graphene devices to aptamers and proteins with PBA is given in Table 2. To the best of my knowledge, this table is as complete a summary as possible of 1-pyrenebutyric acid functionalisation processes for carbon nanotube and graphene field-effect transistor biochemical sensors. By comparing Table 1 and Table 2, it is clear that PBASE is more widely used for non-covalent functionalisation than PBA/EDC. As was the case for PBASE, there are a wide range of process variables used for the functionalisation process, with little justification used for variables chosen. Also notable is the frequent use of polyethylene glycol (PEG) or pyrene-PEG for prevention of non-specific binding (NSB). Non-specific binding is discussed further in ?@sec-non-specific-binding. Despite being less widely used, Mishyn *et al.* [Mishyn2022] state a preference for the use of PBA/EDC over PBASE, as they found it was less prone to hydrolysis and gave a larger reaction yield when binding ferrocene to graphene. A potential downside of using PBA/EDC for protein immobilisation is that EDC has numerous ways of interacting with proteins, and not all of these are necessarily desirable; furthermore, the addition of NHS may also cause other issues, such as precipitation of the reaction compound [Hermanson2013-4]. The greater range of process variables involved in the functionalisation also adds to the complexity of reproducing past results.

### Raman Spectroscopy

Raman spectroscopy was used to verify the attachment of PBA to a carbon nanotube network film with a silicon dioxide substrate in the manner outlined in ?@sec-raman-

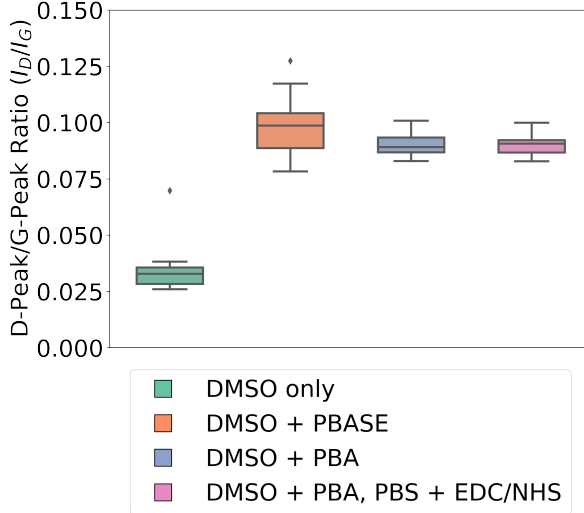


Figure 5: This box plot shows the distribution of D-band peak to G<sup>+</sup>-band peak ratio,  $I_D/I_G$ , across nine locations for a selection of chemically-modified carbon nanotube films. The D-band and G-band intensities for all samples were first normalised to the intensity peak corresponding to the silicon dioxide substrate.

**characterisation.** As highly-bundled devices were found to have less defects present prior to modification, as discussed in ?@sec-pristine-raman, solvent-deposited films were used for the verification of pyrene attachment to prevent the initial presence of defects influencing the analysis. Droplets of DMSO solution were placed on three (solvent-deposited) carbon nanotube films taken from the same wafer. The DMSO solution on one film contained 5 mM PBA, the solution on another film contained 5 mM PBASE, and the DMSO on the final film contained no linker molecule. After incubation for 1 hour, films were rinsed for 15 s with DMSO, then for 15 s with IPA to remove excess DMSO while avoiding hydrolysis of the PBASE. After the first set of Raman spectra was taken, the film initially exposed to PBA was further exposed to a solution of 20 mM EDC and 40 mM NHS in 1XPBS electrolyte for 30 minutes, and a second set of Raman spectra was taken for this film. As in ?@sec-pristine-raman, two spectra taken at each position were processed according to ?@sec-raman-analysis, and the silicon dioxide reference peak measured in the wavenumber range  $100\text{ cm}^{-1} - 650\text{ cm}^{-1}$  was used to normalise the D-band and G-band peaks from the wavenumber range  $1300\text{ cm}^{-1} - 1650\text{ cm}^{-1}$ . The ratio between the average intensity of the D-peak and the G<sup>+</sup>-peak at each position was calculated, and the distribution of ratio values corresponding to each modified film is shown in Figure 5.

There is a  $\sim 3\times$  increase in the intensity ratio  $I_D/I_G$  for both the films modified with PBASE and PBA compared to the film which was only exposed to DMSO. Previous works have found that a change in the intensity ratio indicates successful  $\pi$ -stacking on the carbon nanotube surface, as it indicates surface modification of the carbon nanotubes has occurred [@Wei2010;

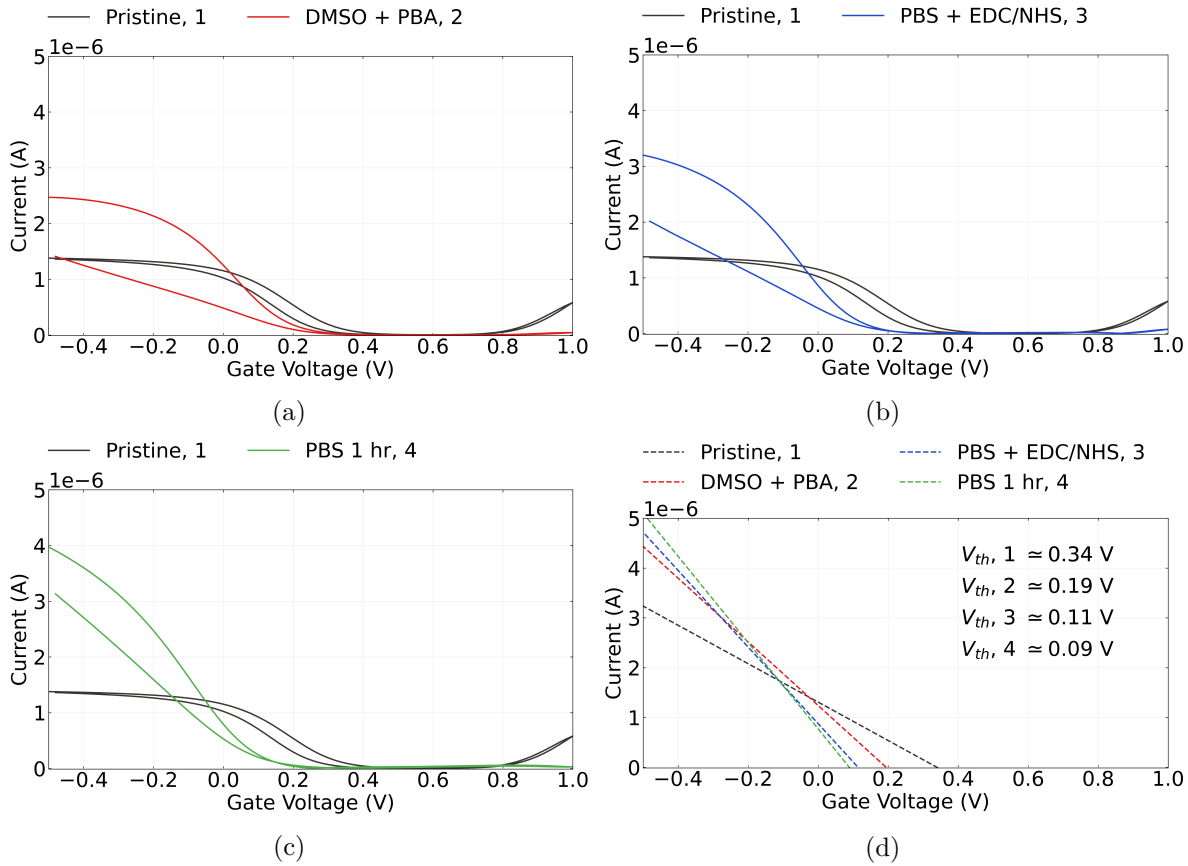


Figure 6: Electrical transfer characteristics of a carbon nanotube transistor before functionalisation alongside the transfer characteristics (a) after being submerged in DMSO containing 5 mM PBA for 1 hour in red, (b) after being submerged in 1XPBS containing 20 mM EDC and 40 mM NHS for 30 min in blue, and (c) after being submerged in fresh 1XPBS for 1 hour in green. The linear fits to the subthreshold slope of each characteristic curve are shown in (d) as dashed lines, alongside the threshold voltages calculated by finding the intercept of each fit.

@Lan2013]. Wei *et al.* [@Wei2010] found functionalisation with PBASE altered the ratio by a factor of  $\sim 1.5\times$ , while Lan *et al.* [@Lan2013] found that functionalisation with PBA altered the ratio by a factor of  $\sim 0.8\times$ . The reason for the large difference between results is not immediately clear, but may result from the significant differences in the pristine composition and morphology of carbon nanotube networks used in each publication, and differences in the functionalisation method used. Across all scan locations in ?@fig-raman-comparison, the value found for  $I_D/I_G$  is consistently  $\sim 0.095$  for both PBA and PBASE. Furthermore, subsequent Raman measurements of the PBA-modified film after further functionalisation with EDC/NHS do not show a significant change in  $I_D/I_G$ . These results indicate that presence of the NHS ester has little effect on the Raman shift. It should be clarified that Raman spectroscopy cannot be used to distinguish between the presence of PBA and PBASE on the device surface. However, it is clear that functionalisation of the carbon nanotube network with both the PBA and PBASE has led to measurable *pi*-stacking between the network and the pyrene group attached to each compound.

## Electrical Characterisation

Figure 6 shows the transfer characteristics of a carbon nanotube transistor channel at various stages of a PBA/EDC functionalisation, where a excess of N-hydroxysuccinimide (NHS) was added alongside EDC. A solvent-deposited carbon nanotube film was used for the device. The PBA was dissolved in DMSO, and the device channels were exposed to this solution for 1 hour. The electrical change resulting from PBA exposure is shown in Figure 6a. The threshold shift with the addition of 5 mM PBA in DMSO for 1 hour is equivalent to the shift seen when only DMSO is added,  $\Delta V = -0.15$  V. The lack of a significant threshold shift directly attributable to the PBA is a result of pyrene having a neutral charge state; any contributions from the charged carboxyl group are screened from the carbon nanotube sidewalls by surrounding water molecules [@Lerner2012]. However, as in the case of the addition of PBASE, there also appears to be an increase in hole mobility, which may be due to the pyrene groups increasing connectivity within the carbon nanotube network [@Murugathas2019b].

Subsequently, the device was rinsed with 1XPBS and exposed to 20 mM EDC and 40 mM NHS in 1XPBS electrolyte for 30 minutes. Figure 6b shows the change resulting from subsequent EDC/NHS exposure. When EDC/NHS is added, a threshold shift of  $\Delta V \sim -0.08$  V was observed on multiple channels. The exposure to EDC/NHS negatively shifts the transfer characteristic curve, most likely due to the PBA present reacting to form positively-charged *O*-acylisourea esters and negatively gating the attached carbon nanotube network [@Heller2008; @Hermanson2013-4]. Figure 6c shows that this shift is not significantly affected by further exposure of the channel to PBS. This indicates that hydrolysis over the course of one hour is insufficient to hydrolyse a significant proportion of the *O*-acylisourea back to PBA, as PBA is charge neutral. We therefore expect that the a significant amount of *O*-acylisourea remains active within this time period and available for reaction with biomolecule amine groups.

## **Attachment of PEGylated Pyrene-Based Linkers**

### **Pyrene-NTA, Pyrene-Biotin and PEGylation**

Through chemical coupling/conjugation, it is possible to replace the NHS ester group on PBASE with other groups that can undergo binding reactions with proteins. Unlike PBASE, these groups do not suffer the drawback of being readily hydrolysed. For example, PBASE can be modified with  $\text{N},\text{N}$ -Bis(carboxymethyl)-L-lysine hydrate (also known as N-(5-Amino-1-carboxypentyl)iminodiacetic acid, AB-NTA) to produce pyrene-nitrilotriacetic acid (pyrene-NTA). The attached NTA group is able to chelate with metal ions such as  $\text{Cu}^{2+}$  or  $\text{Ni}^{2+}$ , which then can then coordinate with polyhistidine-tags attached to a protein [@Holzinger2011; @Amano2016; @Chang2017]. Use of  $\text{Cu}^{2+}$  ions over  $\text{Ni}^{2+}$  gives stronger histidine bonding and less non-specific adsorption [@Chang2017]. Functionalisation using the NTA- $\text{Ni}^{2+}$  chemistry was successfully used to attach mammalian odorant receptors to a single carbon nanotube for detection of eugenol vapour in real-time [@Goldsmith2011]. Pyrene-biotin (pyrene butanol biotin ester) can also be produced for attaching avidin or streptavidin [@Holzinger2011]. As avidin and streptavidin are tetrameric, they can be attached to both pyrene-biotin and biotinylated avi-tagged proteins simultaneously via strong non-covalent bonding, therefore linking the transducer and receptor [@Star2003a; @Dundas2013; @Hermanson2013-11; @Fairhead2015]. As the presence of his-tags and avi-tags on proteins can be readily controlled, these methods offer improved specificity and directionality over the traditional amide bonding seen earlier.

It is also possible to attach polyethylene glycol (PEG) chains to a pyrene group and modify them with reactive groups such as NTA and biotin to attach proteins in the manner outlined in the previous paragraph [@Hermanson2013-18; @Meran2018]. Once modified with PEG, the water solubility of pyrene linkers increases, making it possible to perform a full functionalisation procedure exclusively in aqueous solution [@Hermanson2013-18]. By setting the length of the PEG chain, the size of the linker molecule can be controlled - selection of a short chain is important for ensuring attached receptors remain within the Debye length of the transducer [@Shkodra2021]. Functionalisation of a graphene transducer with pyrene-PEG-biotin has previously been used to bind streptavidin to a graphene field-effect transistor device [@Miki2019]. The PEGylated linkers used in the following sections were purchased pre-prepared. Pyrene-PEG-NTA (2 kDa) was purchased from Nanocs, while pyrene-PEG-FITC (2 kDa, 10 kDa), pyrene-PEG-rhodamine (3.4 kDa), mPEG-Pyrene (10 kDa) and pyrene-PEG-biotin (10 kDa) were purchased from Creative PEGworks.

## **Identifying Functionalisation Issues using Fluorescence Microscopy**

### **General Overview**

Various dyes and fluorescent tags were used to investigate approaches for identifying successful attachment of biomolecules to a carbon nanotube or graphene surface with fluorescence mi-

croscopy. The dyes included fluorescein isothiocyanate (FITC), Rhodamine B and Cyanine 3 (Cy3). Green fluorescent protein was also used for this testing process. It is important to note that these dyes and the GFP chromophore all contain benzene rings which are able to  $\pi$ -stack with carbon rings to some degree [Nakayama-Ratchford2007; Tang2012; Khrenova2019; Qiu2019]. However, there is also significant variation in the effectiveness of this  $\pi$ -stacking, as shown by Figure 7. Here, a clear, specific interaction is seen between Rhodamine B and graphene, but little interaction between FITC and graphene is observed, even when a longer exposure time is used. Whether the addition of pyrene linker groups these dyes, or dye-modified biomolecules, was therefore investigated in further detail. This process then led to the identification of multiple issues that could impede a successful device functionalisation.

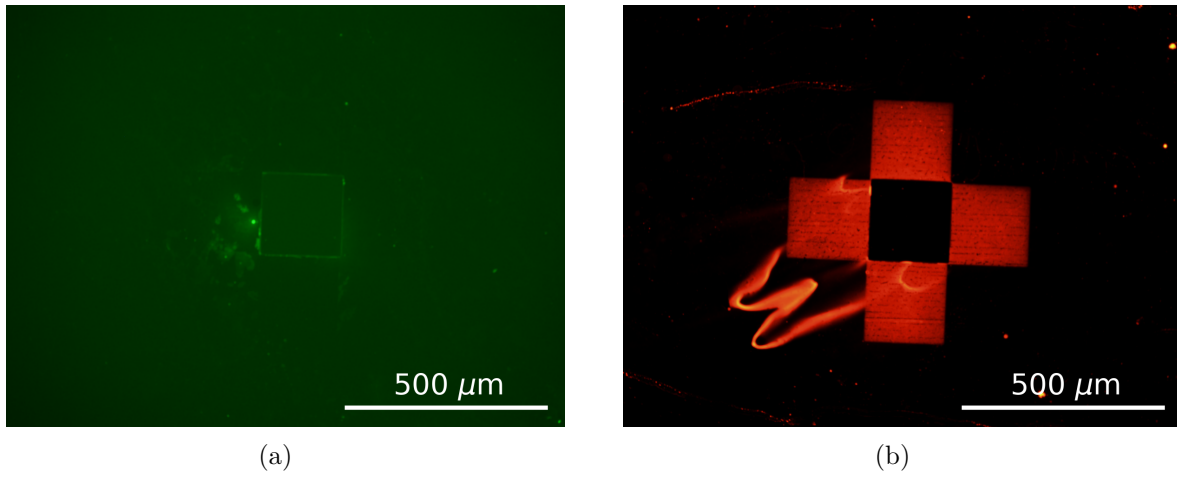


Figure 7: Four 200  $\mu\text{m}$   $\times$  200  $\mu\text{m}$  graphene squares modified with the dyes (a) fluorescein isothiocyanate (FITC) and (b) Rhodamine B. No pyrene/PEG/pyrene-PEG was attached to these dyes. In (a), an FITC filter and 6.5 s exposure time was used, and in (b) a Texas Red filter and 1.4 s exposure time was used.

Both SU8 and AZ® 1518 photoresist fluoresced under a variety of microscope filters, resulting from light interacting with the photoactive component present in both resists [Pai2007]. This background fluorescence was found to drown out fluorescence from a dye-functionalised device channel, and so photoresist encapsulated devices were not used for fluorescence imaging. (Consider a photograph of a dim outdoor lamp; if the photograph was taken on a starless night, the light from the lamp would show up clearly, but with the sun out the light would be very difficult to see regardless of how the photograph was taken.) A different type of encapsulation could potentially be used to verify linker attachment with fluorescence after a device has been encapsulated. These alternative encapsulation methods for use with fluorescence microscopy are discussed in ?@sec-future-work.

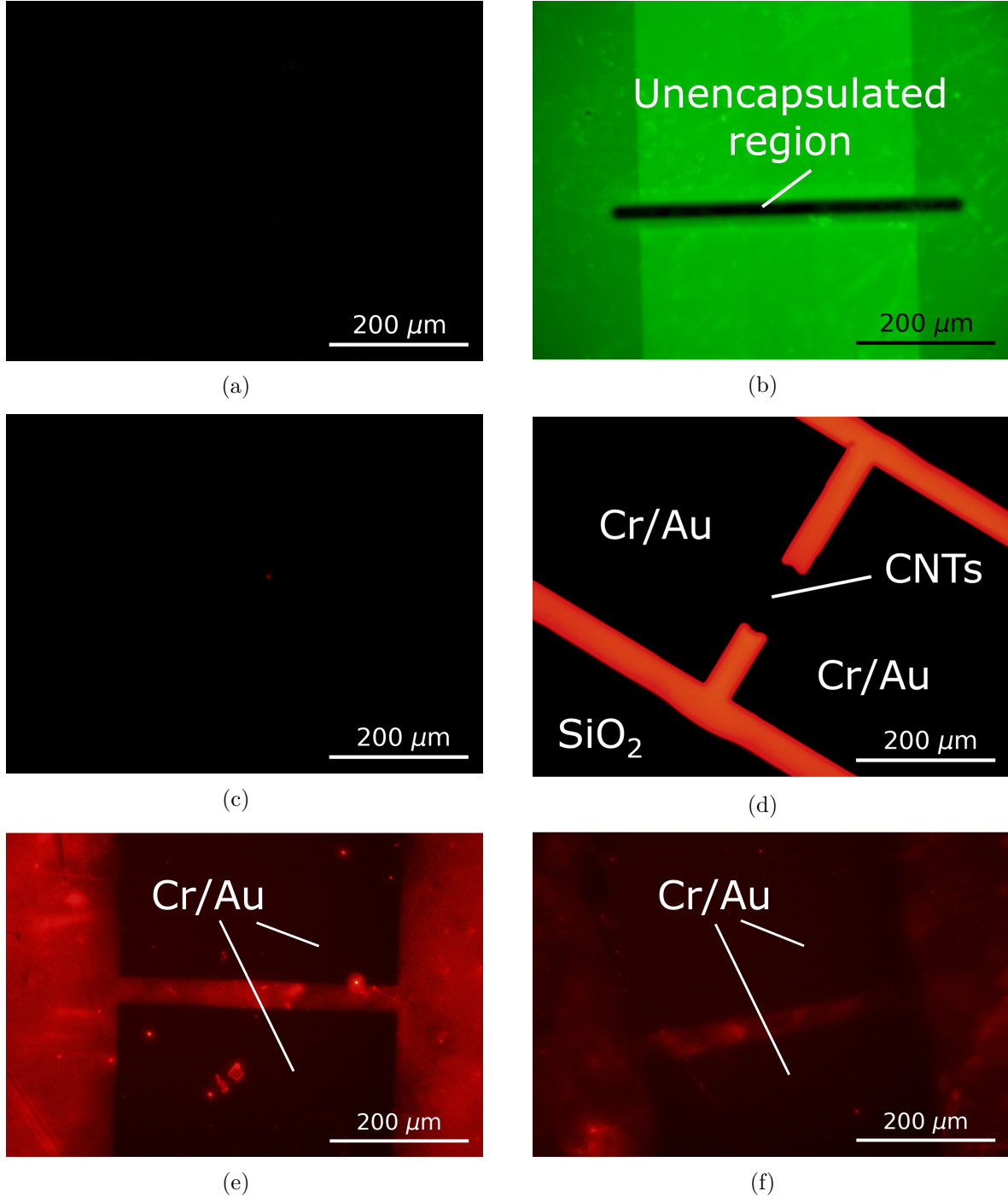


Figure 8: A fluorescence image of a SU8-encapsulated carbon nanotube device is shown in (a), while (b) shows the same channel after modification with a solution of 1 mM Pyrene-PEG-FITC. A 0.35 s exposure time and FITC filter were used for (a)-(b). The fluorescence image in (c) shows an unencapsulated channel, while (d) shows the same channel after Cy3-tagged aptamer exposure. A 10 s exposure time and mCherry filter were used for (c)-(d). The fluorescence images in (e) and (f) show devices precoated with a thin layer of photoresist, then submerged in Cy3-tagged aptamer, where the device in (f) was hardbaked before aptamer exposure. An mCherry filter and 30 s exposure time were used for (e)-(f).

## Photoresist Contamination

An functionalisation issue quickly encountered when characterising pyrene-PEG-FITC (PPF) interaction with sensing channels via fluorescence microscopy was an unwanted secondary interaction between the linker and residual photoresist. Figure 8a and Figure 8b are fluorescence images of SU8 encapsulation (using the pre-2023 mask) before and after being exposed to PPF. Despite the same microscope settings being used to take the images (filter, ISO, contrast, exposure time), the SU8 exposed to PPF appears much brighter than the pristine SU8. This result indicates that the linker appears to have an extensive interaction with the photoresist via an unknown mechanism. No fluorescence is seen from the device channel. The length of exposure time required to see fluorescence from the modified channel would lead to fluorescence from the modified linker attached to the photoresist — as well as the photoresist itself — flooding the image with light. Therefore, it is not clear whether the carbon nanotubes have been functionalised with the dye-modified linker. However, out of caution we can assume that the presence of this secondary interaction is not desirable.

A similar interaction was seen between AZ® 1518 photoresist and fluorescent-tagged, amine-terminated aptamer. An unencapsulated carbon nanotube network device, fabricated using the pre-June 2022 process outlined in ?@sec-fabrication, was incubated with 500 nM Cy3-tagged aptamer in Tris buffer at 4°C overnight. The aptamer was first denatured by heating in a water bath at 95°C for 5 minutes then cooling in an ice bath for 10 minutes before use.

Figure 8c and Figure 8d are fluorescence images of the device channel region before and after exposure to aptamer. A thick red ring is visible around the electrodes after functionalisation, despite no PBASE being used to tether the amine-terminated aptamer. It appears that these bright patches correspond to patches of residual photoresist which have not been completely removed from the carbon nanotube square by the development process. These patches have then interacted with the aptamer, causing them to appear bright under the fluorescence microscope. Beyond potentially interfering with functionalisation, photoresist residue blocking a device channel will prevent interaction with the buffer and prevent sensing.

To test whether residual resist could be prevented from interacting with aptamer by crosslinking the resist, two unencapsulated devices were prepared as follows. Devices were first spin-coated with AZ® 1518 in the manner described in ?@sec-fabrication. Next, the majority of resist was removed by soaking the device in acetone for 1 minute. This process left a thin coating of photoresist on the devices. One of these devices was then hardbaked at 200°C for 1 hour. Both devices were subsequently functionalised in the following manner:

1. Unencapsulated device was submerged in 1 mM PBASE in methanol solution for 1 hour.
2. The device was then rinsed with methanol and Tris buffer.
3. 1  $\mu$ M Cy3-tagged aptamer was denatured by heating in a water bath at 95°C for 5 minutes then cooling in an ice bath for 10 minutes before use.
4. The device was incubated with aptamer in Tris buffer at 4°C overnight.

Fluorescence microscope images of channels from each device are shown in Figure 8e and Figure 8f, where the latter is the device hardbaked before functionalisation. By comparing the two images, it is apparent that hardbaking the AZ® 1518 photoresist significantly reduces the amount of fluorescent aptamer attached to the surface. This result is an indication that sufficient heating of the photoresist can prevent it interacting with PBASE or amine-tagged biological material. However, there is still some Cy3-tagged aptamer fluorescence visible in Figure 8f. It appears that hardbaking has not completely prevented photoresist from interacting with the aptamer. It is possible that heating from the bottom of the device is insufficient to hardbake the photoresist layer completely, an effect that would be amplified for the thick photoresist layer on encapsulated devices. Therefore, from June 2023 onwards devices were vacuum annealed for 1 hour at 150°C prior to functionalisation. This approach was taken to ensure photoresist was heated from above as well as below and made chemically inert across its surface.

This result demonstrates the use of fluorescence microscopy as a tool to detect residue and test suitable residue elimination measures. Further testing showed that performing a 1 minute flood exposure (for positive resist only) then placing a device in AZ® 326 developer for 3 minutes was highly effective at removing photoresist residue. Both these development and annealing techniques were used for all functionalised devices in subsequent sections.

### Hydrophobicity of Carbon Nanotubes and Graphene

As PEGylated linker dissolves well in aqueous solution, initial fluorescence imaging focused on functionalising devices with these linkers dissolved in 1XPBS. It was hoped that by keeping the device channels in a pH-controlled environment, the channel surface would be made more suitable for the attached receptors. Figure 9a shows a graphene film after exposure to pyrene-PEG-rhodamine (PPR) in 1XPBS solution for 1 hour. The pyrene-PEG-rhodamine has interacted with the silicon dioxide substrate (discussed further in Section ) but not the graphene film. The graphene has not attached to the pyrene or rhodamine due to the highly hydrophobic graphene surface repelling the surrounding solution, preventing  $\pi$ -stacking from occurring. The hydrophobicity of the graphene surface is not intrinsic to graphene, but instead results from a hydrocarbonaceous layer which forms on the channel surface when exposed to air [@Ashraf2014]. A hydrophobic layer will also form on carbon nanotube networks [@Stando2019; @Park2022]. Treatment with oxygen plasma at 5 W for 15 s has previously been found to remove this hydrocarbonaceous layer, restoring the intrinsic hydrophilicity of graphene [@Shin2010]. Storing the graphene surface in deionised water rather than air prevents the return of this hydrocarbon layer [@Ashraf2014]. The use of a relatively low power plasma ensures damage to the graphene layer is minimised.

Treatment of an unencapsulated carbon nanotube network device at 5 W for 15 s at 300 mTorr greatly reduced the contact angle of a water droplet placed on the device surface, shown inset in Figure 9 before and after plasma treatment. A graphene film was then functionalised with pyrene-PEG-rhodamine in 1XPBS in the same manner as for the film in Figure 9a, except

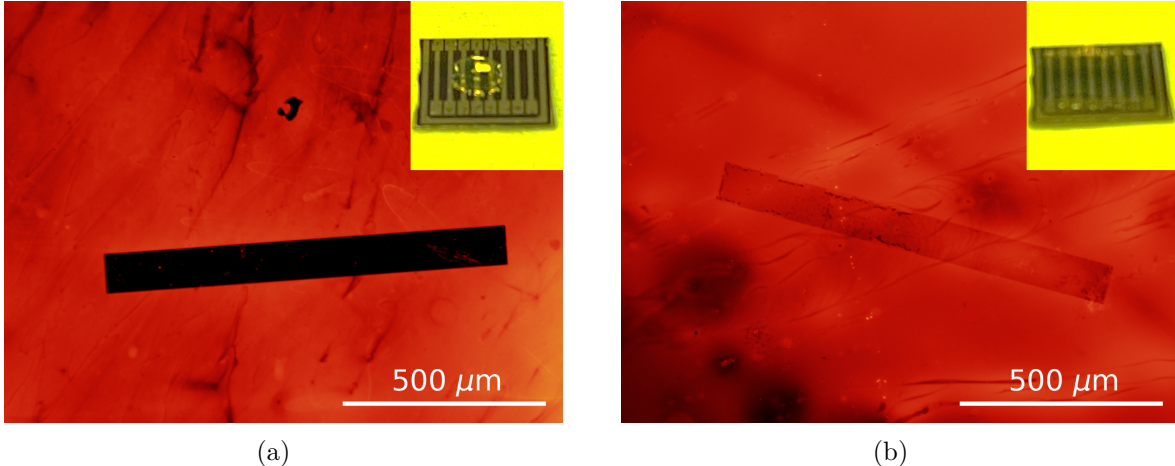


Figure 9: Fluorescence images of a  $1000 \mu\text{m} \times 100 \mu\text{m}$  graphene channel after functionalisation with 1 mM pyrene-PEG-rhodamine in 1XPBS. The graphene film in (a) was not oxygen plasma cleaned before functionalisation, while the graphene film in (b) was oxygen plasma cleaned at 5 W for 15 s at 300 mTorr pressure immediately before functionalisation. Insets show a  $10 \mu\text{L}$  droplet placed on an unencapsulated carbon nanotube device before (a) and after (b) the same oxygen plasma treatment procedure. Images were taken using a Texas Red filter and a 1.8 s exposure time.

with the same plasma treatment performed on the film less than 1 minute before functionalisation. The result is shown in Figure 9b. The graphene now appears to interact with the pyrene-PEG-rhodamine. These results both indicate that the plasma treatment is increasing the hydrophilicity of the device surface, improving the ability of pyrene-PEG-rhodamine to  $\pi$ -stack with graphene. The disadvantage of this procedure is that the plasma cleaning introduces defects to the graphene surface which may be undesirable for device electrical behaviour. Furthermore, it was often found that devices functionalised in this manner had their conductance drop significantly after functionalisation, even though plasma treatment itself did not significantly alter device conductance. Solvent was therefore used for the initial linker functionalisation in Section , as it did not require a plasma cleaning step for successful attachment.

### Substrate Interaction with Linker Molecules

Another issue that arose when verifying surface functionalisation was the interaction between pyrene linker and the silicon dioxide substrate. This interaction meant it was difficult to discern whether the pyrene group was interacting in a specific manner with the channel film. It was confirmed that pyrene-PEG was interacting with silicon dioxide, rather than residual photoresist or nanomaterial, by performing a pyrene-PEG-rhodamine functionalisation on pristine

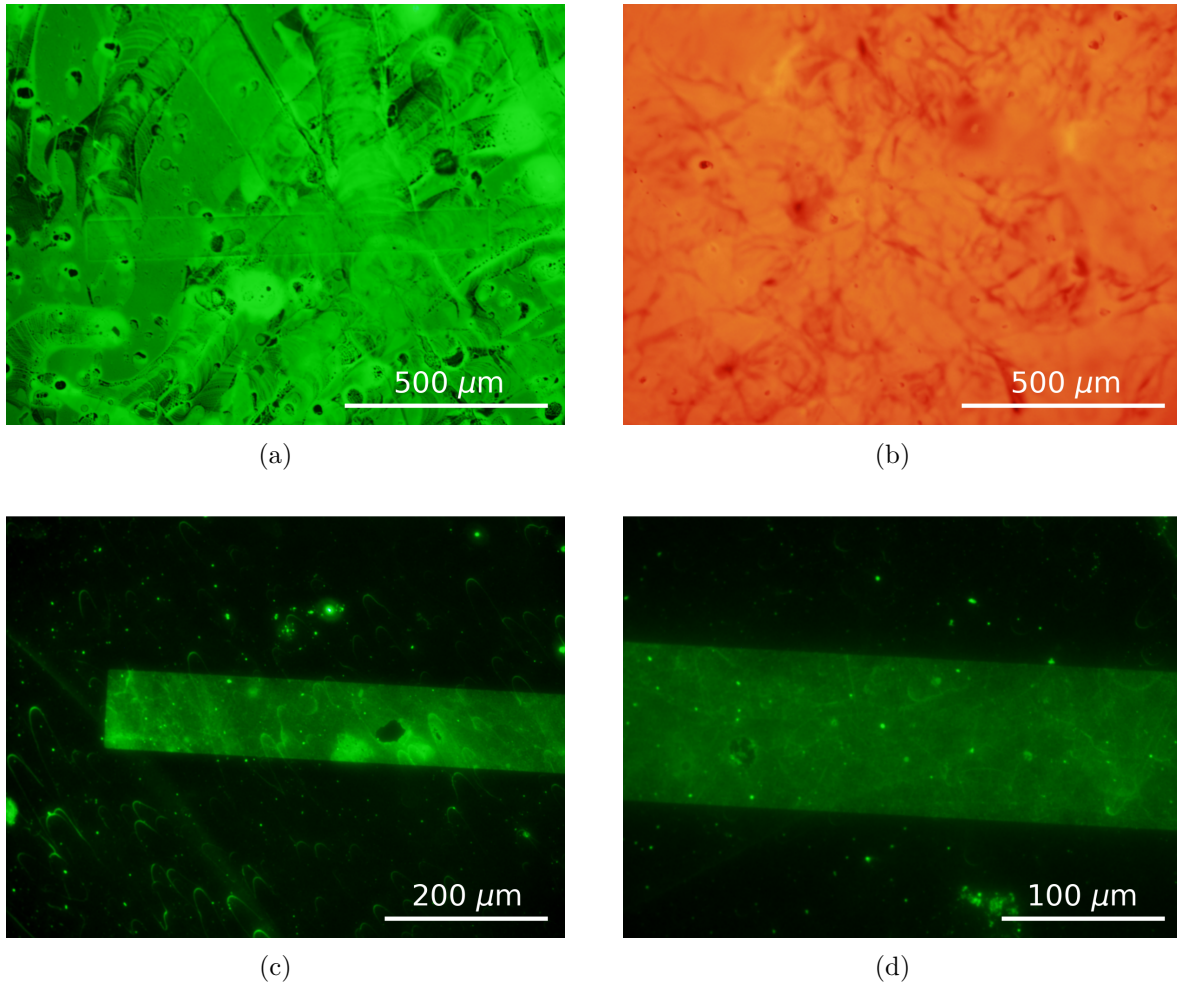


Figure 10: The  $1000 \mu\text{m} \times 100 \mu\text{m}$  graphene film in image (a) was functionalised with 1 mM pyrene-PEG-FITC in 1XPBS after oxygen plasma treatment, taken using an FITC filter and a 1.6 s exposure time. (b) shows a silicon dioxide surface which had never been exposed to carbon nanotubes, graphene or photoresist after exposure to 1 mM pyrene-PEG-rhodamine in 1XPBS, taken using a Texas Red filter and a 1.8 s exposure time. Graphene films on a substrate functionalised with 1 mM pyrene-PEG-FITC in 1XPBS after oxygen plasma treatment then cleaned with m-CNT dispersion surfactant (NanoIntegris) are shown in (c) and (d), where a FITC filter was used, with 7.5 s and 7.75 s exposure times respectively.

silicon dioxide, as shown in Figure 10b. The PEGylated linker supplier suggested that the surface should be thoroughly rinsed with surfactant to remove weakly-bound pyrene-PEG-FITC attached to the silicon dioxide, while preserving the pyrene-PEG-FITC strongly attached via  $\pi$ -stacking to the graphene or carbon nanotube film [CreativePEGworks2022]. The following process was then used to remove pyrene-PEG-FITC from the silicon dioxide: the film was rinsed with DI water for 30 s, then placed in m-CNT dispersion solution (NanoIntegris) for 5 minutes at 70°C while agitating with a pipette, and finally rinsed with DI water, ethanol, acetone, IPA and nitrogen dried. The results of this thorough cleaning process are shown in Figure 10c and Figure 10d. The majority of pyrene-PEG-FITC was removed in regions with no graphene, but remained where graphene was present, indicating specific,  $\pi$ -stacking interaction took place between the pyrene-PEG-FITC and graphene. However, this surfactant rinse step was not used when performing functionalisation with biological materials, to prevent damage to the lipid membranes used.

### Coffee-Ring Effect

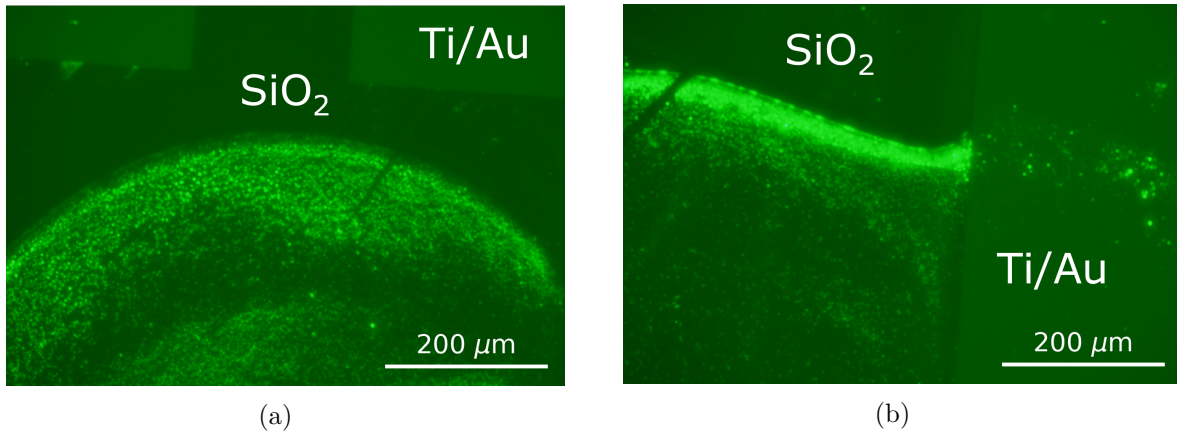


Figure 11: Both (a) and (b) show a build-up of his-tag GFP at the edges of the droplet region where pyrene-PEG-NTA had been present, taken using an GFP filter and a 5 s exposure time. On the right hand side of (b), no his-tag GFP is visible on the metal electrode, as no pyrene-PEG attaches to the metal electrodes.

From Table 1, full device submersion appears to be the most common approach for functionalisation with solution containing linker molecules like PBASE. However, some groups placed small droplets of solution onto the device channels when functionalisation, and this approach was tested as part of the fluorescence verification work. For functionalisation with his-tagged green fluorescent protein, after plasma cleaning at 5 W for 15 s at 300 mTorr, a 4  $\mu$ L droplet of 100  $\mu$ M pyrene-PEG-NTA in 1XPBS was placed on each graphene device channel and left covered in a humid environment for 15 minutes. The device was then rinsed with 1XPBS, submerged in 10 mM NiSO<sub>4</sub> in 1XPBS for 1 hour, rinsed in 1XPBS, then submerged in 10

mL of 100 ng/mL his-tag GFP solution (Thermofisher) overnight. Fluorescence microscope imaging showed that a ring of biomaterial would build up around the outer edge of regions where pyrene-PEG-NTA had been present, as seen in Figure 11.

It appears this is a result of the his-tag GFP attaching to a dense region of pyrene-PEG-NTA at the edge of the functionalisation droplet. This accretion of pyrene-PEG-NTA at the edge of the droplet is a result of the coffee-ring effect, where the evaporation of the droplet leads to transport of particles to the droplet edges via capillary flow [@Deegan1997; @Shimobayashi2018]. As this gradient in surface coverage of attached proteins has unknown consequences for sensing, in subsequent sections devices were functionalised with PBASE or pyrene-PEG-NTA by submerging them in solution instead of dropcasting.

### Verifying Linker-OR Nanodisc Attachment with Fluorescence Microscopy

To verify the formation of amide (or imide) bonds between PBASE and the odorant receptors (ORs) contained within nanodiscs, a fluorescent biomarker was directly attached to the odorant receptors for detection with fluorescence microscopy. The biomarker used was the *Aequorea Victoria* green fluorescent protein (GFP). As far as I know, this is the first time fluorescence has been used to verify the successful attachment of odorant receptor nanodiscs to a carbon nanotube network.

The functionalisation of unencapsulated carbon nanotube devices (steam-deposited, fabricated using post-June 2023 methods outlined in ?@sec-fabrication) with PBASE and GFP-OR nanodiscs was performed as follows:

1. The device was exposed to UV light for 1 minute, placed in AZ® 326 developer for 3 minutes, then rinsed with acetone, isopropanol and nitrogen dried.
2. The device was vacuum annealed for 1 hour at 150°C (Note: Steps 1 & 2 were added to ensure any residual photoresist on the channel was removed or passivated before functionalisation, see Section ).
3. A solution of 1 mM PBASE (Setareh Biotech) in methanol prepared by fully dissolving 2 mg PBASE in 5 mL methanol by vortex mixing at 1000 rpm in a dark room (Note: PBASE was stored at -18°C for 18 months prior to use, and was thawed under vacuum for 15 minutes in dark conditions before opening)
4. The device was then rinsed with methanol, fully submerged in ~ 1 mL of PBASE in methanol solution and left covered with parafilm for 1 hour, then rinsed with methanol for 15 s, rinsed with 1XPBS for 15 s and nitrogen dried to remove residual PBASE.
5. The device was left dry and in darkness while collecting the GFP-OR nanodiscs from the -80°C freezer.

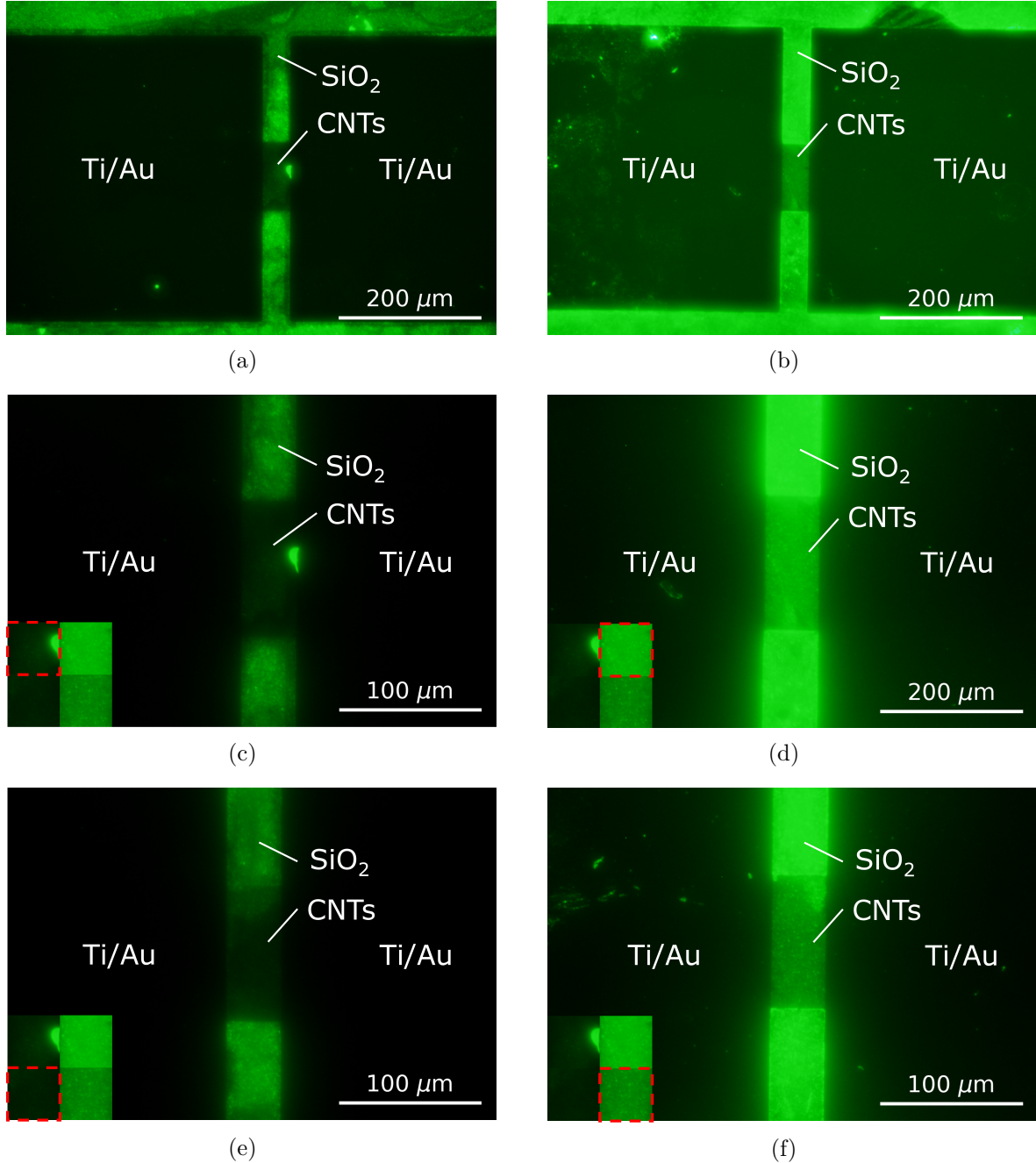


Figure 12: The fluorescence images on the left side – (a), (c) and (e) – show unencapsulated carbon nanotube network channels from a device incubated in GFP-OR43b nanodiscs. The fluorescence images on the right – (b), (d) and (f) – show the channels of a similar device after successive PBASE and GFP-OR43b nanodisc incubation. Images (a) and (c) are both of the same channel on the first device, and images (b) and (d) are of the same channel on the second, but (c) and (d) were taken using a greater magnification. The insets in (c)-(f) compare the central channel region of (c)-(f) more directly. All images were taken using the same microscope settings, with a GFP filter and a 10 s exposure time.

6. 20  $\mu$ L GFP-OR nanodiscs (batch number ND-GFP-OR43b-0002, prepared 12 months earlier) were diluted in 2 mL 1XPBS (Note: The full 2 mL was used to flush out the nanodisc vial when preparing the nanodisc solution, with successive additions and subtractions of 50  $\mu$ L 1XPBS into and from the vial).
7. The device was submerged in the GFP-OR43b nanodisc solution and left covered with parafilm for 1 hour, then rinsed with 1XPBS for 15 s.
8. For fluorescence microscopy, the device was briefly rinsed with DI water and nitrogen dried to remove dried-down salt residue left by the 1XPBS.
9. Fluorescence microscope images were taken immediately after functionalisation; devices were transported to the fluorescence microscope room in a foil-wrapped container, and the fluorescence microscope room was kept dark while images were taken.

A control device was prepared using the same process but skipping steps 3 and 4. Fluorescence images of both devices are shown in Figure 12. All fluorescence images were taken of channels with a measured resistance within a 50-500 k $\Omega$  range both before and after functionalisation.

As mentioned in ?@sec-fluorescence-characterisation, the rectangular dark regions to the left and right of each image are the gold electrodes. The silicon dioxide regions in each image appear bright under the GFP filter, indicating non-specific binding between the GFP-OR43b nanodiscs and the silicon dioxide substrate. As this device has been annealed, UV exposed and developed before functionalisation, this non-specific attachment is unlikely to be interaction with residual photoresist (see Section ). The SiO<sub>2</sub> substrate also appears brighter in the images on the right of Figure 12, which are of the device initially exposed to PBASE. The discussion in Section indicates that the pyrene moiety of PBASE may non-specifically interact with the silicon dioxide substrate, therefore, the SiO<sub>2</sub> substrate may have had a coating of attached PBASE when the device on the right of Figure 12 was submerged in the GFP-OR43b nanodiscs. The attachment of GFP-OR43b nanodiscs to this PBASE coating may have been more extensive than direct attachment of GFP-OR43b nanodiscs to the silicon dioxide, which led to brighter fluorescence of the modified silicon dioxide for the PBASE-incubated device.

A comparison of fluorescence in the channel region between images on the left of Figure 12 (GFP-OR43b only) and the images on the right (GFP-OR43b and PBASE) is given by the inset in Figure 12c-f. The inset demonstrates that the channels not incubated in PBASE are significantly less bright than those that had been incubated with PBASE. It appears that, as expected from the discussion in Section , the GFP-OR43b in 1XPBS is unable to approach the unmodified channel due to the hydrophobicity of the carbon nanotubes. However, when the carbon nanotubes are modified with PBASE, the GFP-OR43b is able to attach to the channel, and so the channel shows up brightly under the fluorescence microscope GFP filter. This trend was consistent across all conducting channels on each of the two devices.

## Conclusion

It has been well-established in the literature that the  $\pi$ -stacking reaction mechanism between pyrene-based linkers and graphene and carbon nanotube network field-effect transistors can be used to create working biosensors. The previous use of various linker molecules for biosensor functionalisation was investigated. Despite the wide use of 1-pyrenebutanoic acid N-hydroxysuccinimide ester (PBASE) and 1-pyrenebutyric acid (PBA) for functionalisation of biosensors, the literature shows a significant variation in the methods used for attachment of linker molecules to a transistor channel. The most common methods, using 6 mM PBASE dissolved in dimethylformamide or 1 mM PBASE in methanol, stem directly from the first documented use of PBASE for functionalisation of carbon nanotube biosensors. In the last 6 years, more research has been done into optimising the PBASE methodology for graphene devices, but there is still disagreement in the literature over whether minimising or maximising PBASE coverage on a graphene device channel is desirable for sensing. Due to disagreement in the literature around suitable non-covalent methods for biosensor functionalisation, several steps were taken to identify a rapid and simple method for verifying successful functionalisation, and to locate any potential barriers to a successful functionalisation.

I first compared the advantages and disadvantages of the various linker molecules under investigation. The use of hydrogen NMR gave indications that water was present in PBASE samples prepared in DMSO. Concerns around the impact of the hydrolysis of PBASE on functionalisation mean that the presence of water is strongly undesirable. An alternative functionalisation approach less prone to hydrolysis is the reaction of PBA with EDC in the presence of NHS. However, this process has its own disadvantages, such as undesirable protein interactions and the increased amount of steps and process variables involved. Pyrene-NTA is also less prone to hydrolysis than PBASE but unlike PBASE or PBA/EDC interacts with a specific protein tag, the histidine tag. PEGylation of the pyrene-NTA linker also means that the entire functionalisation process can be performed in aqueous solution, avoiding the introduction of non-organic solvents. This approach is desirable, since the non-aqueous solvents traditionally used for functionalisation may have negative impacts on device behaviour. For example, carbon nanotube device channel transfer characteristics were found to undergo a significant shift of  $\Delta V = -0.15 \pm 0.02$  when exposed to DMSO or MeOH for 1 hour.

Next, I verified that the pyrene groups of the linker molecules of interest were attaching successfully to either carbon nanotubes or graphene. Raman spectroscopy showed that incubating a highly-bundled carbon nanotube film in 5 mM PBASE or PBA in DMSO for 1 hour increased  $I_D/I_G$  by a factor of  $\sim 3$  relative to the DMSO-only case. Incubating a steam-deposited carbon nanotube device in a 1 mM concentration of PBASE in methanol or DMSO for 1 hour was found to cause a significant increase in device on-current relative to the solvent-only case, and a similar increase in on-current was seen for 5 mM PBA in DMSO relative to the DMSO-only case. When a PBA-functionalised device was placed in aqueous solution with 20 mM EDC and 40 mM NHS for 30 minutes, a further increase in on-current was seen. Fluorescence microscopy was used to demonstrate the successful attachment of pyrene-PEG to graphene

using an attached FITC probe, where immersing a graphene film in 1 mM pyrene-PEG in ethanol led to the channels becoming brightly fluorescent relative to the background using a 1 s exposure time.

Various obstacles to successful functionalisation were encountered and addressed. Photoresist contamination was addressed with exposure and development steps before functionalisation (no exposure for SU8 encapsulated devices). Hydrophobicity of graphene films was addressed by plasma treatment before functionalisation in aqueous solution. A surfactant rinse was used to distinguish between weak substrate-linker interaction and  $\pi$ -stacking between linker and the channel. Finally, coffee-ring distribution of linker was addressed by always submerging the device in linker when functionalising.

Finally, fluorescence microscopy was used to investigate PBASE functionalisation of GFP-tagged odorant receptors. An eight-channel device was modified by submersion in 1 mM PBASE in methanol for 1 hour, then submersion in  $10 \mu\text{L mL}^{-1}$  OR43b nanodiscs in 1XPBS for 1 hour. An eight-channel control device was also prepared by submersion in  $10 \mu\text{L mL}^{-1}$  OR43b nanodiscs in 1XPBS for 1 hour, but with no PBASE. The channels of the PBASE-submersed devices showed significant GFP fluorescence, while the channels of the control devices showed little to no GFP fluorescence. As far as I am aware, this is the first time fluorescence has been used to verify successful attachment of odorant receptors to a carbon nanotube network.